A Molecular Beacon Strategy for the Thermodynamic Characterization of Triplex DNA: Triplex Formation at the Promoter Region of Cyclin D1[†]

Thomas Antony,[‡] Thresia Thomas,[§,||,#] Leonard H. Sigal,[‡,⊥] Akira Shirahata,[×] and T. J. Thomas*[,‡,#]

Departments of Medicine, Environmental and Community Medicine, Pediatrics, and Molecular Genetics and Microbiology, The Cancer Institute of New Jersey, and Environmental and Occupational Health Sciences Institute, University of Medicine and Dentistry of New Jersey-Robert Wood Johnson Medical School, New Brunswick, New Jersey 08903, and Faculty of Pharmaceutical Sciences, Josai University, Sakado, Saitama 350-02, Japan

Received February 26, 2001

ABSTRACT: We studied the formation of triplex DNA in the purine−pyrimidine-rich promoter site sequence of cyclin D1, located at −116 to −99 from the transcription initiation site, with a molecular beacon comprised of a G-rich 18-mer triplex forming oligodeoxyribonucleotide. Formation of triplex DNA was monitored by enhanced fluorescence of the beacon, due to the weakening of fluorescence energy transfer, upon its binding to the target duplex. Electrophoretic mobility shift assay confirmed triplex DNA formation by these oligonucleotides. In low salt buffer (10 mM Na^+), triplex DNA formation was not observed in the absence of a ligand such as spermine. At room temperature (22 °C), the equilibrium association constant (K_a) calculated in the presence of 1 μM spermine and 10 mM Na^+ was 3.2×10^8 M^{-1}. The K_a value was 1.0×10^9 M^{-1} in the presence of 150 mM Na^+, and it increased by 10-fold by the addition of 1 mM spermine. ΔH, ΔS, and ΔG of triplex DNA formation, calculated from the temperature dependence of K_a in the range of 20−45 °C, were −35.9 kcal/mol, −77 cal/(mol·K), and −13 kcal/mol, respectively, in the presence of 150 mM NaCl. The corresponding values were −52.9 kcal/mol, −132.5 cal/(mol·K), and −13.4 kcal/mol in the presence of 150 mM NaCl and 1 mM spermine. Structurally related polyamines exerted different degrees of triplex DNA stabilization, as determined by binding constant measurements. Comparison of spermine versus hexamine showed a 17-fold increase in the equilibrium association constant, whereas bis(ethyl) derivatization lead to a 4-fold decrease of this value. In the absence of added duplex and polyamines, the molecular beacon dissociated with a melting temperature of 67 °C. Thermodynamic parameters of beacon melting were calculated from the melting curve, and the ΔH, ΔS, and ΔG values were 37.8 kcal/mol, 112 cal/(mol·K), and 4.4 kcal/mol, respectively. These results demonstrate that molecular beacons can be used for the direct determination of the equilibrium association constants and thermodynamic parameters of triplex DNA formation in the presence of ligands such as polyamines.

Molecular beacons are a new class of nucleic acid probes that make use of sequence-specific interaction of nucleic acid bases and the phenomenon of fluorescence energy transfer. They are designed to have a stem and loop structure with a fluorescent molecule (donor) and a nonfluorescent quencher (acceptor) attached to the 5′ and 3′ ends, respectively, of an oligonucleotide (*1*, *2*). When the donor and acceptor are in close proximity, they share electrons and can form a transient complex that dissipates the energy as heat (*2*). In a stable stem and loop structure, the donor and acceptor are close enough to exchange the energy and are nonfluorescent or weakly fluorescent. However, when the donor and acceptor molecules are far apart and unable to exchange energy, as in a linear structure, the beacon becomes fluorescent. Molecular beacons have been successfully employed in many applications, including the detection of RNA, real time detection of RNA·DNA and DNA·DNA hybrids in living cells, and DNA sequence analysis (*3*−*7*). The ability of molecular beacons to differentiate mutated sequences from wild-type sequences offers a unique role for these molecules to identify various mutant strains in diseases such as tuberculosis (*8*, *9*).

We have been interested in studying the formation and stabilization of triplex DNA for gene therapy applications (*10*, *11*). With an increasing understanding of the role of specific genes in tumorigenesis, several approaches have been developed to regulate the expression of disease-related genes

[†] This work was supported, in part, by the National Cancer Institute through NIH Grants CA73058, CA80163, and CA42439 and a Grant-in-Aid for Scientific Research from the Ministry of Education, Science, and Culture of Japan.

* To whom correspondence should be addressed at the Clinical Academic Building, Room 7090, 125 Paterson Street, UMDNJ-Robert Wood Johnson Medical School, New Brunswick, NJ 08903. Phone: (732) 235-8460. Fax: (732) 235-8473. E-mail: thomastj@UMDNJ.edu.

[‡] Department of Medicine, University of Medicine and Dentistry of New Jersey-Robert Wood Johnson Medical School.

[§] Department of Environmental and Community Medicine, University of Medicine and Dentistry of New Jersey-Robert Wood Johnson Medical School.

[||] Environmental and Occupational Health Sciences Institute, University of Medicine and Dentistry of New Jersey-Robert Wood Johnson Medical School.

[#] The Cancer Institute of New Jersey, University of Medicine and Dentistry of New Jersey-Robert Wood Johnson Medical School.

[⊥] Departments of Pediatrics and Molecular Genetics and Microbiology, University of Medicine and Dentistry of New Jersey-Robert Wood Johnson Medical School.

[×] Faculty of Pharmaceutical Sciences, Josai University.

10.1021/bi010397z CCC: $20.00
Published on Web 07/12/2001

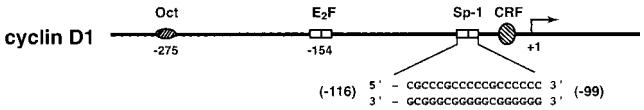

FIGURE 1: Promoter region map of cyclin D1, showing the G-rich region target of the TFO.

(*14*−*18*). Transcriptional suppression of genes by stable triplex DNA formation at the promoter sites of such genes is an antigene strategy with potential therapeutic implications (*10*−*13*). The triplex DNA technology is directed to inactivate a target gene by a suitably designed oligonucleotide that can bind to the target duplex through the major groove by Hoogsteen or reverse Hoogsteen hydrogen bonding (*14*, *15*). Cyclin D1 is one of the key cell cycle regulators, overexpressed in a wide variety of human neoplasms, including breast cancer (*19*, *20*). Overexpression of cyclin D1 is suggested to deregulate cell proliferation and induce tumorigenesis (*21*, *22*), suggesting that cyclin D1 plays an important oncogenic role. Kim and Miller (*23*) have identified an 18 nucleotide long purine.pyrimidine rich motif in cyclin D1 promoter, located at −116 to −99 from the transcription initiation site, which is capable of forming triplex DNA with a triplex forming oligonucleotide (TFO)[1] oriented antiparallel to the purine-rich strand. This site is also the SP1 binding region (Figure 1), and the in vitro inhibition of SP1 binding by a TFO suggests the possibility of targeting cyclin D1 for antigene therapeutics (*23*).

Several experimental techniques have been used to investigate triplex DNA formation, including melting temperature (T_m) measurements, circular dichroism (CD) spectroscopy, electrophoretic mobility shift assay (EMSA), affinity cleavage assay, and filter binding assay (*24*−*27*). Yang et al. (*28*) and Aich et al. (*29*) have used the fluorescence resonance energy transfer (FRET) and polarization measurements to directly determine triplex DNA binding constants. In this technique, the donor and acceptor molecules are fluorescent and are attached to the TFO and one of the duplex strands, respectively. The emission spectrum of the donor overlaps with that of the acceptor and the transfer of energy occurs as a result of dipole−dipole coupling between the donor and acceptor. As a modification to FRET technique, we propose a molecular beacon approach in which the molecular beacon binds to the duplex DNA and forms the triplex DNA in which the donor and acceptor are no longer in close proximity due to the opening of the stem structure to single stranded form, thereby leading to enhanced fluorescence.

To determine the binding affinity of a TFO targeted to the promoter region sequence of cyclin D1, we designed a molecular beacon that exhibited very low fluorescence emission because of energy transfer between the donor and acceptor molecules. There was a 20-fold increase in the fluorescence emission intensity when this beacon bound to the target duplex. We used this increase in fluorescence emission intensity to determine the association constant of

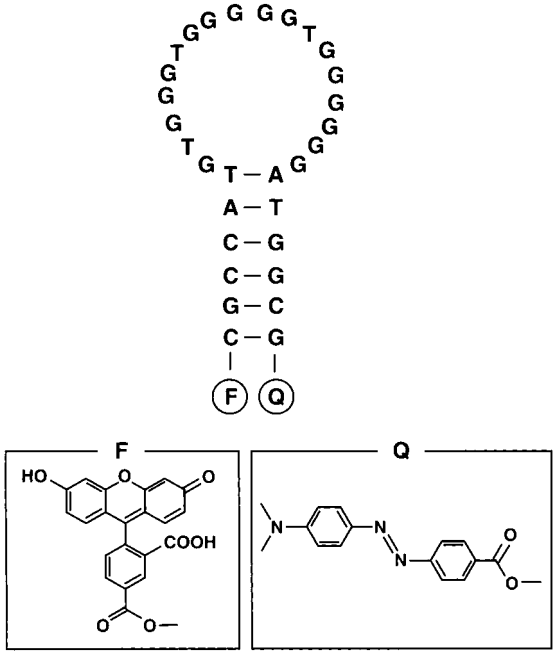

FIGURE 2: Structure of the molecular beacon used in this study, with an 18-nucleotide loop region containing the cyclin D1 TFO. F (Fluorescein) and Q (DABCYL) are the fluorescent donor and acceptor (quencher), respectively.

the TFO with its target and evaluate thermodynamic parameters associated with triplex DNA formation. In addition, we used this technique to evaluate the efficacy of the natural polyamine, spermine ($H_2N(CH_2)_3NH(CH_2)_4NH(CH_2)_3NH_2$) and its synthetic analogues to stabilize the triplex DNA structure at the cyclin D1 promoter region sequences.

EXPERIMENTAL PROCEDURES

Oligonucleotides. The molecular beacon and the target duplex DNA strands were purchased from Research Genetics, Inc. (Birmingham, AL). The synthesis of the beacon molecule involved first the synthesis of modified synthetic oligonucleotides containing a primary amino group covalently attached to the 3′ end and a sulfhydryl group protected by a trityl moiety covalently attached to the 5′ end (*30*). The quencher, 4-([4′-(dimethylamino)phenyl]azo)benzoic acid (DABCYL) was coupled to the 3′ end of the oligonucleotide. The oligonucleotide was then purified by high-pressure liquid chromatography (HPLC), the protective group was removed, and a fluorescein molecule (donor) was conjugated to the reduced thiol (*1*, *2*). The molecular beacon possessing both fluorophore and quencher moieties was purified by HPLC, lyophilized, and used in our experiments. The structure of the molecular beacon used in our study is shown in Figure 2. The molar concentration of the molecular beacon was calculated from UV absorption measurements at 260 nm using the following molar extinction coefficients for each of the bases: 15.4 (A), 11.8 (G), 7.4 (C), and 9.6 (T) $mM^{-1}\cdot cm^{-1}$. The extinction coefficient of the beacon, calculated according to the nearest neighbor approximation (*31*), was 332.6 $mM^{-1}\cdot cm^{-1}$. Both fluorescein and DABCYL absorb at 260 nm with extinction coefficients of 9.6 and 10.24 $mM^{-1}\cdot cm^{-1}$, respectively; however, their contribution to the calculated molar concentration of the beacon oligonucleotide is negligible (<6%).

[1] Abbreviations: TFO, triplex forming oligonucleotide; T_m, melting temperature; CD, circular dichroism; EMSA, electrophoretic mobility shift assay; FRET, fluorescence resonance energy transfer; DABCYL, 4-([4′-(dimethylamino)phenyl]azo)benzoic acid; HPLC, high-performance liquid chromatography; 3−4−3, spermine; 3−3−3−3, 1,15-diamino-4,8,12-triazapentadecane; 3−4−3−4−3, 1,21-diamino-4,9,-13,18-tetraazahenicosane; BE, bis(ethyl).

Table 1: Nucleotide Sequence of Oligonucleotides Used in This Study

oligonucleotide	nucleotide sequence	ϵ, $mM^{-1}\cdot cm^{-1}$ [a]
TFO	5′-GTGGGTGGGGGTGGGGGG-3′	205.8
specific duplex (30-mer)	5′-CCCCTGCGCCCGCCCCCGCCCCCCTCCCGC-3′	248.4
	3′-GGGGACGCGGGCGGGGGCGGGGGGAGGGCG-5′	339.2
control duplex I	5′-CCGCCCCGCTCCCGCCCTCCCGCCCGCCCC-3′	248.4
	3′-GGCGGGGCGAGGGCGGGAGGGCGGGCGGGG-5′	339.2
control duplex II	5′-CCGCGCGGCCCTGCGCCGCTCGGCGCGGCC-3′	279.2
	3′-GGCGCGCCGGGACGCGGCGAGCCGCGCCGG-5′	308.4
c-erbB-2 duplex	5′-CCCTCCTCCTCCACCTCCTCCTTCTCCT-3′	235.0
	3′-GGGAGGAGGAGGTGGAGGAGGAAGAGGA-5′	360.6
c-myc duplex	5′-CTCCTCCCCACCTTCCCCACCCTCCCCACCCTCCC CA-3′	319.0
	3′-GAGGAGGGGTGGAAGGGGTGGGAGGGGTGGGA GGGGT-5′	449.4

[a] ϵ values were calculated by the nearest neighbor approximation method (*31*).

Control oligonucleotides were purchased from Oligos, Etc. (Wilsonville, OR). These oligonucleotides were of the HPLC level I purification grade and certified to contain >90% full length oligonucleotide by capillary electrophoresis analysis. The remaining material was mainly n-1 and n-2 length oligonucleotides. Each oligonucleotide was checked for integrity by 5′-radiolabeling, followed by gel electrophoresis. [γ-^{32}P]ATP was purchased from NEN Life Science Products, Inc. (Boston, MA), and T-4 polynucleotide kinase, from Life Technologies, Inc. (Rockville, MD.) We used the 30-mer target duplex of the TFO and control duplexes for examining the binding of the molecular beacon to form the triplex DNA. Additional controls included the purine−pyrimidine-rich promoter region sequences of c-*myc* and c-*erb*B-2 oncogenes (*31*−*33*). The nucleotide sequence and extinction coefficients of the oligonucleotides used in this study are given in Table 1.

Polyamines. Spermine·4HCl was purchased from Sigma Chemical Co. (St. Louis, MO). The polyamine analogues 1,15-diamino-4,8,12-triazapentadecane (3−3−3−3, $H_2N(CH_2)_3NH(CH_2)_3NH(CH_2)_3NH(CH_2)_3NH_2$) and 1,21-diamino-4,9,13,18-tetraazahenicosane (3−4−3−4−3, $H_2N(CH_2)_3NH(CH_2)_4NH(CH_2)_3NH(CH_2)_4NH(CH_2)_3NH_2$) were synthesized and characterized as described earlier (*34*). Bis(ethyl)-spermine (BE−3−4−3, $H_5C_2HN(CH_2)_3NH(CH_2)_4NH(CH_2)_3NHC_2H_5$) and BE−3−3−3−3 were also synthesized by methods previously described (*34*). (These compounds are abbreviated by a number system using the number of methylene groups between the primary and secondary amino groups.) The chemical structure and purity of the synthesized compounds were determined by elemental analysis, NMR, HPLC, and mass spectrometry. Stock aliquot (20 mM) of the polyamines were prepared in deionized and distilled water, and appropriate dilutions were made for each experiment.

Preparation of Triplex DNA. Duplex DNA was first prepared by annealing equimolar concentrations of the corresponding single strands. The target or control duplex, molecular beacon, and appropriate concentrations of polyamines were incubated for 5 min in a water bath at 95 °C, cooled to room temperature, and incubated for 16 h at 22 °C before use in fluorescence measurements. The buffer used was 10 mM Na cacodylate (pH 7.4) with or without NaCl.

Fluorescence Measurements. The fluorescence measurements were carried out using a Fluoromax-2 spectrofluorometer (Instruments SA, Edison, NJ). All the measurements were done at room temperature (22 °C), except for the temperature-dependent fluorescence measurements. The buffer used was 10 mM Na cacodylate, pH 7.4, containing 0.5 mM EDTA, unless otherwise specified. Fluorescence emission spectra were recorded between 495 and 700 nm upon excitation at 485 nm with a bandwidth of 5 nm for the excitation and emission. A cylindrical quartz cuvette with volume capacity of 350 μL was used for these measurements. The experimental concentration of the molecular beacon was 10 nM, and that of the duplex target varied from 1 to 500 nM.

For fluorescence measurements at different temperatures, a water-jacketed cell holder was used. The temperature of the cell holder was controlled by a NESLAB (Portsmouth, NH) water bath (model RTE 111) with a temperature sensor attached to the sample chamber. For the measurement of thermodynamic parameters using ln K_a versus $1/T$ plots, triplex DNA was preformed and incubated overnight as described earlier and kept at the desired temperature for 30 min to attain equilibrium, before taking the readings. The increase in fluorescence intensity leveled off in ~10 min of mixing the oligonucleotides (ODNs). The reversibility of the dissociation of triplex DNA and the beacon was studied by heating/cooling at a rate of 0.5 °C/min. The triplex DNA stabilized by NaCl/spermine was stable up to 45 °C and then dissociated to beacon structure. The melting temperature of the beacon was determined to be 67 °C in the presence of 150 mM NaCl. To eliminate any effect from the beacon dissociation in the evaluation of thermodynamic parameters of triplex DNA, the isothermal measurements were done between 15 and 45 °C. These measurements were carried out in a standard 1 cm quartz cuvette.

Melting Temperature (T_m) Measurement. The T_m measurements of the triplex DNA and beacon molecule were done at a heating rate of 0.5 °C/min, with the fluorescence emission intensity at 515 nm and temperature recorded every 30 s. The cooling curve of the beacon was obtained by decreasing the temperature at a rate of 0.5 °C/min and recording the fluorescence intensity at 515 nm as a function of temperature. Fluorescence−temperature profiles of the triplex DNA and beacon molecule were recorded in 10 mM Na cacodylate buffer (pH 7.4), containing 140 mM NaCl. The melting profile of the triplex DNA was also generated under the same buffer and NaCl concentration with 1 mM spermine. T_m values were taken as the temperatures corresponding to half-dissociation of the triplex/duplex/beacon, and the reproducibility was within 1 °C between individual experiments.

Calculation of Equilibrium Association/Dissociation Constant and Thermodynamic Parameters. The binding of duplex (D) and the single-stranded TFO (S) to form a triplex DNA

(T) can be represented as:

$$D + S \rightleftarrows T \quad (1)$$

At equilibrium, the association constant (K_a) is given by

$$K_a = [T]/[D][S] = 1/K_d \quad (2)$$

where K_d is the dissociation constant of the triplex DNA.

In the molecular beacon experiment, the fluorescence emission intensity of fluorescein increases on triplex DNA formation due to linearization of the beacon structure and the removal of the acceptor moiety (DABCYL) away from fluorescein to prevent energy transfer. In our experiment, the concentration of the duplex is increased while that of the beacon is kept constant. At any given concentration of the duplex, the observed intensity

$$I_{obs} = I_S + I_T \quad (3)$$

where I_S and I_T are the fluorescence intensities of the unbound and bound (in the form of triplex DNA) beacon, respectively. Concentration of the triplex at any concentration of duplex is calculated from the fluorescence emission intensity using the equations where $[S_0]$ is the total concentration of beacon and I_{obs}, $I_S°$, and I_T^∞ are the observed fluorescence emission intensity and that of the free and totally bound beacon, respectively.

$$[T] = \{[I_{obs} - I_S°]/[I_T^\infty - I_S°]\}[S_0] \quad (4)$$

$$I_{obs} = I_S° + \frac{[I_T - I_S°][T]}{[S_0]} \quad (5)$$

If "α" is the fraction of beacon that is converted to triplex DNA, eq 2 can be written as

$$K_d = \{([D_0] - \alpha[S_0])([S_0] - \alpha[S_0])\}/\alpha[S_0] \quad (6)$$

where $[D_0]$ is the total concentration of the duplex. Expanding the equation,

$$\alpha = \{b - (b^2 - 4[S_0][D_0])^{1/2}\}/2 \quad (7)$$

where $b = [D_0] + [S_0] + K_d$. Since $[T] = \alpha[S_0]$, substituting for T in eq 5 results in

$$I_{obs} = I_S° + \frac{[I_T^4 - I_S°]}{2[S_0]}\{b - (b^2 - 4[S_0][D_0])^{1/2}\} \quad (8)$$

K_d is determined by fitting the above equation to the I_{obs} vs $[D_0]$ curve using the Sigmaplot software.

The free energy of triplex DNA formation (ΔG) at room temperature (22 °C) was calculated from the standard relation $\Delta G = -RT \ln K_a$, where R is the universal gas constant and T is the absolute temperature.

The thermodynamic parameters ΔH, ΔS, and ΔG of triplex DNA formation were determined from the temperature dependence of equilibrium association constant of triplex DNA formation. ΔH and ΔS were determined from the slope and intercept of $\ln K_a$ vs $1/T$ plot according to the equation $\ln K_a = -(\Delta H/RT) + \Delta S/R$.

Molecular beacon contains a loop structure and a stable stem formed by Watson−Crick base pairing of the complementary nucleotides. We determined the thermodynamic parameters of the beacon stem melting using a procedure described by Bonnet et al. (*35*). According to this method, the dissociation constant of the beacon (K_d^b) is represented by the equation

$$K_d^b = \{(F - \beta)/(\gamma - F)\} \quad (9)$$

where F is the observed fluorescence intensity at a given temperature and β and γ are the fluorescence intensities of the beacon in the closed and open forms, respectively. The values of β and γ were measured at 15 and 80 °C, respectively. Since $\Delta G = -RT \ln K_a = \Delta H - T\Delta S$ and $K_d = 1/K_a$,

$$R \ln\{(\gamma - F)/(F - \beta)\} = -\Delta H/T + \Delta S \quad (10)$$

Using this relationship, ΔH and ΔS were determined from the slope and intercept of a plot of $R \ln\{(\gamma - F)/(F - \beta)\}$ versus $1/T$. In these equations, R is the gas constant and T is the absolute temperature (K).

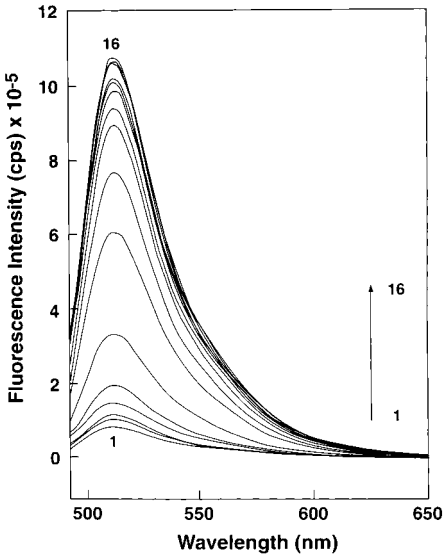

FIGURE 3: Fluorescence emission spectra of the molecular beacon at different concentrations of target duplex in 10 mM Na cacodylate buffer, pH 7.4, containing 0.5 mM EDTA and 140 mM NaCl. The concentration of the duplex increased from 0 to 100 nM (1−16: 0, 0.1, 0.25, 0.5, 1, 2.5, 5, 7.5, 10, 15, 20, 25, 37.5, 50, 75, and 100 nM). Concentration of the molecular beacon was 10 nM. All measurements were performed at 22 °C.

Electrophoretic Mobility Shift Assay (EMSA). The purine-rich strand of the duplex was 5′-end labeled with [γ-^{32}P]-ATP and then annealed to its complementary pyrimidine-rich strand by heating at 90 °C for 10 min and cooling overnight. The duplex target was incubated with the TFO and appropriate concentrations of the polyamine analogue (*3−4−3−4−3*) in binding buffer containing 20 mM Tris-borate (pH 7.8) and 5 mM $MgCl_2$. Samples were incubated overnight at 37 °C, separated by electrophoresis on 10% native polyacrylamide gels at 150 V in 90 mM Tris-borate (pH 7.8) and 5 mM $MgCl_2$, and analyzed by autoradiography.

RESULTS

Triplex DNA Formation in the Presence of 150 mM NaCl. Figure 3 shows the results of our fluorescence studies on the binding of the molecular beacon to its 30-mer duplex DNA target in cacodylate buffer with 150 mM Na^+. The

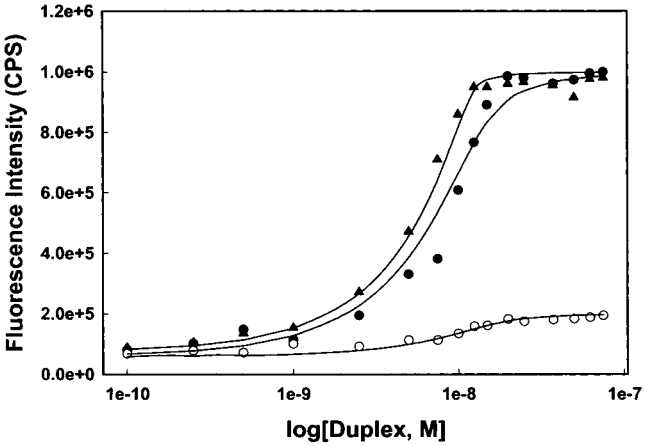

FIGURE 4: Plots of fluorescence emission intensity of molecular beacon at 515 nm and 22 °C with increasing concentration of target duplex. The experimental conditions were the following: 10 mM Na^+ (○); 150 mM Na^+ (●); 150 mM Na^+ + 1 mM spermine (▲) The solid lines are the fitted curves according to eq 8 given in the text.

Table 2: Equilibrium Association Constants of Triplex DNA Formation at 22 C

Na^+, mM	polyamine (concn)	K_a, M^{-1} [a]
10	none	b
	3−4−3 (spermine) (1 μM)	3.2×10^8
	BE−3−4−3 (1 μM)	7.2×10^7
	3−3−3−3 (1 μM)	1.4×10^9
	BE−3−3−3−3 (1 μM)	3.6×10^8
	3−4−3−4−3 (1 μM)	5.3×10^9
150[c]	none	1×10^9
	3−4−3 (spermine) (1 mM)	1×10^{10}
	3−3−3−3 (1 mM)	7.9×10^9

[a] K_a values were calculated from fluorescence intensity versus duplex concentration plots generated at 22 °C. Average values from 2 to 4 measurements are presented. The reproducibility was within 10%. [b] No triplex DNA formation was observed in the presence of 10 mM Na cacodylate buffer. [c] For increase of the Na^+ concentration to 150 mM, 140 mM NaCl was added to the 10 mM Na cacodylate buffer.

molecular beacon is weakly fluorescent in the buffer and in the presence of low concentrations of duplex; however, its emission intensity increased with duplex concentration and stabilized at ~20-fold higher intensity, as compared to that of the beacon alone. The fluorescence intensity versus duplex concentration plot showed that, in the presence of 150 mM NaCl, the beacon binding was saturated at a duplex concentration of $\sim 4 \times 10^{-8}$ M, i.e. beacon to duplex molar ratio of 4 (Figure 4). The triplex DNA binding constant calculated from this plot was $(1.0 \pm 0.6) \times 10^9$ M^{-1} (Table 2).

The fluorescence intensity of the beacon did not change significantly with increased concentrations of the 30-mer duplex in the presence of the 10 mM Na cacodylate buffer alone, suggesting the inability of 10 mM Na^+ alone to support the triplex DNA formation. To determine whether the binding of the molecular beacon to the duplex target was sequence specific, we used 4 control sequences (Table 1). These included scrambled sequences without and with 7 G → C base substitutions and the G-rich promoter region sequences of c-*myc* and c-*erb*B-2 promoters. In all cases, there was no increase in the intensity of the beacon when mixed with these duplexes up to a concentration of 10^{-6} M in the presence of 150 mM NaCl. (Results not shown. Also please see Figure 5B.)

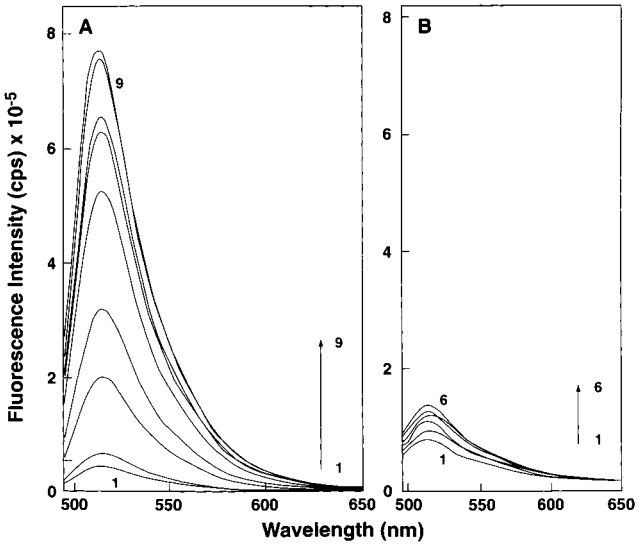

FIGURE 5: Fluorescence emission spectra of molecular beacon at different concentrations of target (A) or nonspecific (control duplex I) (B) duplex in 10 mM Na cacodylate buffer, pH 7.4, containing 0.5 mM EDTA and 1 μM spermine. The concentration of the molecular beacon was 10 nM. Concentrations of duplex in figure A were the following (nM): 1, 0; 2, 1; 3, 5; 4, 10; 5, 20; 6, 50; 7,100; 8, 250; 9, 500. For Figure B, the nonspecific duplex concentrations were the following (nM): 1, 0; 2, 1; 3, 10; 4, 50; 5, 100; 6, 500. Molecular beacon and the target/control duplex were incubated with spermine at 95 °C for 5 min and equilibrated at room temperature for 16 h before use in fluorescence measurements. All measurements were performed at 22 °C.

Effect of Polyamines on Cyclin D1 Triplex DNA Formation. The naturally occurring polyamine, spermine, and its synthetic analogues are known to stabilize triplex DNA formation in both the pyrimidine- and purine-motif triplex DNA models (*36*−*39*). Therefore, we examined the ability of spermine and several structurally related synthetic polyamines to stabilize triplex DNA formation at the cyclin D1 promoter target site using the molecular beacon. Figure 5A shows the effect of 1 μM spermine on the fluorescence intensity of the beacon in the presence of different concentrations of the 30-mer duplex target in 10 mM Na cacodylate buffer. There was a concentration-dependent increase in fluorescence intensity up to 5×10^{-8} M duplex (beacon-to-duplex ratio of 5), beyond which the intensity plateaued. In contrast, there was no increase in the fluorescence intensity from the beacon when the duplex DNA was substituted by a control duplex (Figure 5B). We determined the association constants of cyclin D1 triplex DNA formation in the presence of polyamines, and these values are presented in Table 2. Although there was no indication of triplex DNA formation in Na cacodylate buffer alone, even 1 μM spermine stabilized the triplex DNA with an association constant of 3.2×10^8 M^{-1}. Bis(ethyl)spermine was less effective than spermine in stabilizing triplex DNA formation; however, the pentamine (3−3−3−3) and hexamine (3−4−3−4−3) analogues of spermine were more efficient, with a 17-fold increased association constant in the presence of 3−4−3−4−3 compared to the same concentration of spermine.

Increased stabilization of triplex DNA was also found with spermine in the presence of 150 mM NaCl (Figure 4 and Table 2). There was a 10-fold increase in the association constant in the presence of 1 mM spermine and about 8-fold increase in the presence of the pentamine, 3−3−3−3.

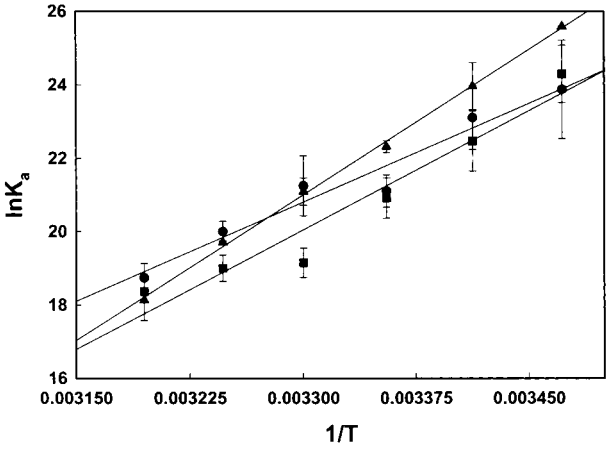

FIGURE 6: Determination of thermodynamic parameters from temperature-dependent association constant values. ΔH was calculated from the slope, and ΔS, from the intercept. The experimental conditions were 150 mM Na^+ (●), 150 mM Na^+ + 1 mM spermine (▲), and 150 mM Na^+ + 1 mM 3−3−3−3 (■).

Table 3: Thermodynamic Parameters of Triplex DNA Association and Beacon Stem Melting

	Na^+, mM	polyamine (concn)	ΔH, kcal/mol	ΔS, kcal/mol	ΔG, kcal/mol
TFO binding[a]	150	none	−35.9	−77	−13.0
	150	spermine, 1 mM	−52.9	−132.5	−13.4
	150	3−3−3−3, 1 mM	−43.4	−103.1	−12.7
beacon stem melting[b]	150	none	37.8	112	4.4

[a] Thermodynamic parameters of TFO (beacon) association with its duplex target were determined from Figure 6, as described in the text. [b] Thermodynamic parameters of the beacon stem melting were determined from Figure 8. The parameters are listed as positive units because the measurements are based on the dissociation of the beacon stem.

To determine the thermodynamic parameters of triplex DNA formation, we next determined the K_a values in the presence of 150 mM NaCl, 150 mM NaCl + 1 mM spermine, and 150 mM NaCl + 1 mM 3−3−3−3 under different (15−45 °C) isothermal equilibrium conditions. Thermodynamic parameters were calculated from the temperature dependence of K_a values, using van't Hoff's plots (Figure 6 and Table 3). ΔH, ΔS, and ΔG values of triplex DNA stabilized by 150 mM NaCl were −35.9 kcal/mol, −77 cal/(mol·K), and −13 kcal/mol. There was a decrease in ΔH and ΔS values when 1 mM spermine was present. For the triplex DNA stabilized by 150 mM NaCl and 1 mM 3−3−3−3, the ΔH, ΔS, and ΔG were −43.4 kcal/mol, −103.1 cal/(mol·K) and −12.7 kcal/mol.

Thermal Denaturation of Triplex DNA and Molecular Beacon. Figure 7 shows a comparison of the melting profile of triplex DNA and the beacon. Triplex DNA was associated with high fluorescence emission because the beacon is present in its linear form. The fluorescence intensity of triplex DNA increased by ~25% upon increasing the temperature from 15 to 45 °C. There was a sharp decrease in the fluorescence intensity between 45 and 52 °C in the case of triplex DNA formed in the presence of 150 mM Na^+, with a T_m value of 48 °C. The decrease in the fluorescence intensity is an indication of the dissociation of the beacon TFO from the duplex and its reconstitution to the closed beacon form. The decrease in the fluorescence intensity occurred between 50 and 60 °C in the case of the triplex

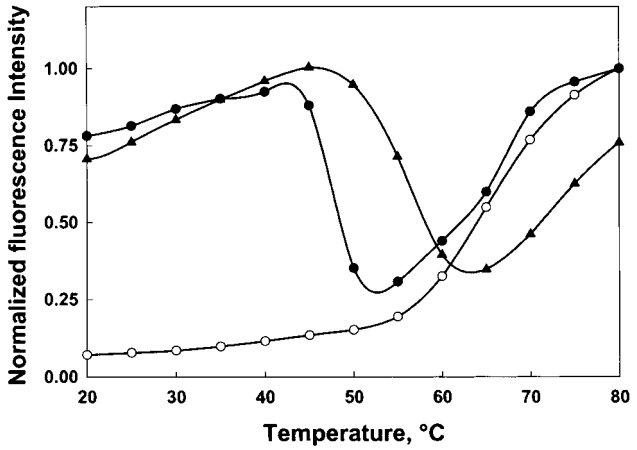

FIGURE 7: Fluorescence−temperature profiles of triplex DNA formed from the molecular beacon (10 nM) and 30-mer duplex target (50 nM) in the absence (●) and presence (▲) of 1 mM spermine. The experiments were performed in 10 mM Na cacodylate buffer containing 140 mM NaCl. The melting profile of the beacon (○) in the absence of duplex DNA (in 10 mM Na cacodylate buffer containing 140 mM NaCl) is also shown for comparison. The fluorescence data were collected at a heating rate of 0.5 °C/min.

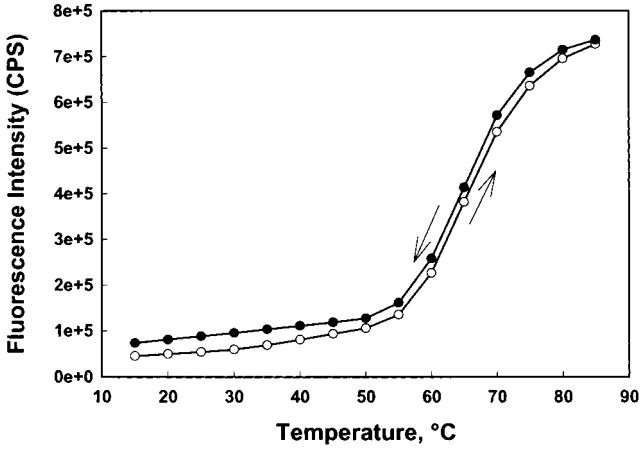

FIGURE 8: Heating (○) and cooling (●) curves of the molecular beacon in 10 mM Na cacodylate buffer containing 140 mM NaCl. Both curves were generated at a rate of 0.5 °C/min.

DNA formed in the presence of 150 mM Na^+ + 1 mM spermine, with a T_m value of 55 °C, indicating the stabilization of cyclin D1 triplex DNA by the polyamine. The fluorescence intensity increased at higher temperatures, indicating the thermal melting of the stem of the beacon molecule. The T_m value of this duplex stem was 67 °C in the presence of 150 mM Na^+. This T_m value was confirmed to be that of the beacon stem by independently performing a melting experiment of the beacon molecule in the presence of 150 mM Na^+. The melting of the stem, however, occurred at a temperature higher than 67 °C in the presence of 1 mM spermine. This result indicates that duplex stem is also stabilized by spermine, a result similar to previous studies on duplex DNA stabilization by polyamines (*40*).

We also examined the reversibility of the duplex stem melting by recording the heating and cooling profiles of the beacon in 10 mM Na cacodylate buffer in the presence of 140 mM NaCl (Figure 8). The heating−cooling curves were nearly superimposable, suggesting the absence of hysteresis phenomenon. Therefore, we determined the thermodynamic

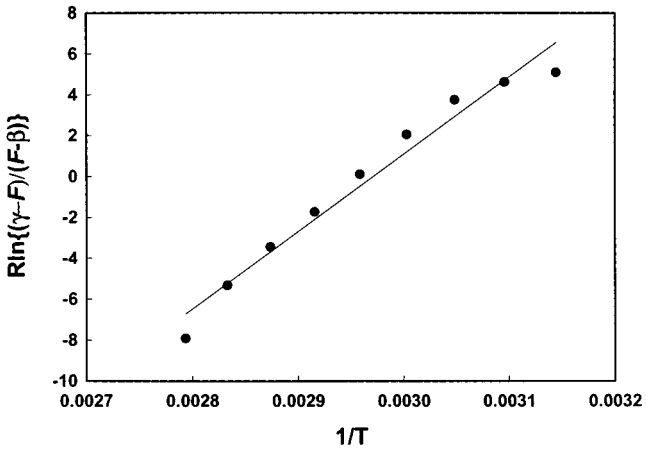

FIGURE 9: Thermodynamic characterization of beacon stem melting. The ΔH and ΔS values were determined from the slope and intercept of a plot of $R \ln\{(\gamma - F)/(F - \beta)\}$ against $1/T$, according to eq 10 in the text.

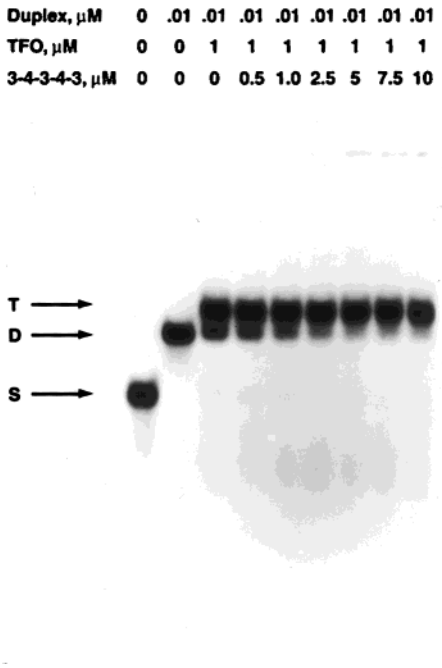

FIGURE 10: Autoradiogram showing the effect of 3−4−3−4−3 on cyclin D1 triplex DNA formation. Lanes 1 and 2 represent the labeled 30-mer purine-rich strand and the duplex, respectively.

parameters of the beacon melting from the slope and intercept of a plot of $R \ln\{\gamma - F)/F - \beta)\}$ against $1/T$ (Figure 9). The calculated values of ΔH, ΔS, and ΔG were 37.8 kcal/mol, 112 cal/(mol·K), and 4.4 kcal/mol, respectively (Table 3).

Triplex DNA Formation Monitored by EMSA. To confirm the triplex DNA formation by cyclin D1 TFO and its duplex target, and its stabilization by polyamines, we used EMSA. Figure 10 shows the triplex DNA formation of the 18-mer TFO with the 30-mer target duplex (TFO to duplex molar ratio = 100) at different concentrations of 3−4−3−4−3. EMSA results show a significant level of triplex DNA formation in the absence of the polyamine analogue in a buffer containing 20 mM Tris-borate and 5 mM $MgCl_2$. Addition of 0.5−5 μM of 3−4−3−4−3 caused an increase in triplex DNA formation, leading to 100% conversion of the labeled duplex to triplex DNA at 5 μM of 3−4−3−4−3.

Since the buffer used for EMSA experiment contained 20 mM Tris-borate and 5 mM $MgCl_2$, we further examined triplex DNA formation under these conditions by fluorescence spectroscopy using the molecular beacon. The binding pattern was the same as observed in the presence of 150 mM NaCl. The fluorescence intensity increased by 15-fold in the presence of 50 nM duplex (beacon-to-duplex ratio = 5) and plateaued thereafter.

DISCUSSION

The data presented in this paper demonstrate the application of a molecular beacon technique for the direct determination of equilibrium association constants and thermodynamic parameters of triplex DNA formation at the cyclin D1 promoter sequence under different environmental conditions. The molecular beacon approach has advantages in the selective determination of ΔH, ΔS, and ΔG of triplex DNA formation at low temperatures (<45 °C) without interference from duplex or the beacon stem. The duplex is nonfluorescent and the dissociation of the beacon stem occurs at a higher temperature (T_m = 67 °C) than that of triplex DNA dissociation. Hence this approach is more useful for determining the thermodynamic parameters of triplex DNA formation than the conventional UV melting studies, in which the difference in the melting temperature of duplex and triplex DNA is rather small and deconvolution to the corresponding melting profiles is often difficult. Moreover, equilibrium conditions are compromised in both melting temperature- and EMSA-based determination of thermodynamic parameters of triplex DNA formation.

The molecular beacon approach may also be more useful than other fluorescence-based approaches, such as FRET and fluorescence polarization measurements to study triplex DNA formation (*28, 29*). Polarization of a fluorescent molecule depends on the rotational flexibility and orientation of the dipole moment of the fluorophore. Therefore a difference in size alone may not necessarily change the polarizability of the molecule significantly. In the FRET approach, TFO and one of the duplex strands have to be fluorescently labeled, and hence, the extension of this technique to cellular applications is not feasible. In contrast, the donor and acceptor tags are present in the same beacon oligonucleotide, and therefore, beacon molecules can be targeted to cellular studies for real-time determination of the third strand hybridization with the genome. The molecular beacon, which is "dark" in the closed state, will be fluorescent or "shining" after its hybridization because of its low background signal.

Triplex DNA formation at the cyclin D1 promoter was previously studied by Kim and Miller (*23*); however, we found the ability of spermine and its analogues to facilitate triplex DNA formation at this target. Positively charged ligands such as the polyamines have a demonstrated stabilizing effect on triplex DNA, partly because of their ability to shield the increased negative charge density created by the association of three DNA strands (*37*−*40*). For example, the phosphate charge distance in single-stranded, duplex, and triplex DNA are 4.3, 1.7, and 1.1 Å, respectively (*40*). The K_a values of the triplex DNA stabilized by spermine, 3−3−3−3, and 3−4−3−4−3 were 3.2×10^8, 1.4×10^9, and 5.3×10^9 M^{-1}, respectively, at 10 mM Na cacodylate buffer. Thus, the "polyamine effect" increases with the number of

positive charges on the polyamine. Bis(ethyl)polyamines are less effective than their nonbisethylated counterparts, a result in conformity with the efficacy of these compounds in stabilizing duplex DNA (*41*). In addition to their positive charge, polyamines also exert structural specificity effects in stabilizing triplex DNA (*37, 42*), suggesting possible contributions from site-specific interactions of polyamines with triplex DNA.

Most of the reported values of the ΔH of triplex DNA are for pyrimidine motif triplex DNA, and the average value is in the range of 2−8 kcal/base for the third strand base hydrogen bonding (*43, 44*). Scaria et al. (*45*) reported ΔH values of 2.4, 4.5, and 3.8 kcal/(mol·base) for 10-mer purine/pyrimidine, purine, and pyrimidine motif triplexes, respectively, from calorimetric determination, showing that the mixed purine/pyrimidine sequences are the least stable. The sequence used in the present study is purine rich but contains three pyrimidine bases also. The average ΔH value obtained per third strand base in the present study (2.4 kcal/(mol·base) for third strand base pair) is also in this range. The decrease in the value of the thermodynamic parameters $\Delta\Delta H$, $\Delta\Delta S$, and $\Delta\Delta G$, 17 kcal/mol, 55.5 cal/(mol·K), and 0.4 kcal/mol, respectively, in the presence of spermine as compared to that in the presence of NaCl is a measure of the triplex DNA stabilizing effect of the polyamine. It is important to note that the difference in ΔG is negligible despite a large decrease in ΔH. This is due to the corresponding decrease in ΔS. This type of enthalpy−entropy compensation is a general property of weak biomolecular interactions (*46*), including DNA melting (*47*), protein unfolding and conformational transitions (*48, 49*), and drug−DNA interactions (*50*). Although the origin of this phenomenon remains obscure, water molecule reorganization around the macromolecule contributes significantly to the enthalpy and entropy changes but little to the free energy change.

The molecular beacon molecule has three parts. The central part is the TFO. The distal parts are mutually complementary and form Watson−Crick double-stranded stem structure when the molecule is free in solution. The stem must melt when the beacon molecule binds to a duplex to form triplex DNA. Therefore, we determined the T_m and thermodynamic parameters of the stem melting (Figures 8 and 9; Table 3). The ΔH value obtained for the beacon stem (6.3 kcal/base pair) is close to the average value for duplex melting (∼6 kcal/mol base pair) (*24, 43, 51*−*53*). Bonnet et al. (*35*) reported the thermodynamic parameters of a beacon stem formed from CGCTC and its complementary strand, and the ΔH, ΔS, and ΔG values reported in that work are comparable to the values determined by us.

It is important to note here that triplex DNA formation between the beacon and the 30-mer duplex used in our study might have involved hydrogen bonding from the stem part also. Opening of the stem and positioning of the bases along the 30-mer duplex target allows the formation of four more CGC triplets and two TAT triplets, which also contributes to the association constant measured in this study. However, the presence of mismatched bases between these sequences reduces their contribution compared to the continuous stretch of triplets formed by the TFO part of the beacon and its target duplex region.

Sequence specificity is an important factor in the success of any antigene or antisense technology (*12*−*15*). Earlier studies on the hybridization of molecular beacons to their complementary and noncomplementary strands using different colored probes showed significant selectivity in the recognition of the specific target by these beacons (*54*). In addition to scrambled sequences with some changes in bases, we used 2 other duplexes, the c-*myc* and c-*erb*B-2 promoter region sequences, as controls. The lack of an increase in fluorescence intensity of the beacon in association with these sequences indicates lack of cross-reactivity between the cyclin D1 TFO and c-*myc* and c-*erb*B-2 gene promoter sequences despite the presence of G-rich sequences in the oligonucleotides. This result is important to design gene specific TFOs for antigene therapeutics.

The presence of a G−C-rich sequence in cyclin D1 makes it a target for the binding of the transcription factor SP1 (Figure 1). Kim and Miller (*23*) showed the binding of cyclin D1 duplex to recombinant SP1 and prevention of the binding on triplex DNA formation. The increased extent of triplex DNA formation in the presence of polyamines, at a fixed duplex:TFO ratio in EMSA (Figure 10), further suggests that polyamine analogues such as 3−4−3−4−3 can be effective secondary ligands to facilitate triplex DNA-mediated transcriptional inactivation.

In the context of the present study, it is important to mention that fluorescence-based techniques are increasingly being employed for studying biomolecular interactions, including the structural and conformational transitions of DNA and protein−DNA interactions because of the sensitivity of the technique and the ease of experimentation. These techniques are fast, very sensitive, nonradioactive, and nondestructive in nature. They can be used for fast and accurate determination of thermodynamic and kinetic parameters of triplex DNA formation (*28, 29*). FRET between donor and acceptor molecules attached to separate linear strands of DNA was found to be a suitable method for studying inter- and intramolecular associations of DNA, like DNA triplex and tetraplex formation (*55*), and for the determination of the orientation of the third strand along the duplex target. Since the concentration of fluorescent probes required is much lower than that necessary for other conventional methods, such as UV, CD and NMR spectroscopy and EMSA, problems associated with intermolecular association are minimized in this technique (*56, 57*).

In conclusion, the results presented in this paper demonstrate the use of a molecular beacon to monitor the formation and stabilization of triplex DNA at a therapeutically important target and to determine the association constants of TFO/duplex binding. This technique also allows the measurement of triplex DNA melting temperature, determination of thermodynamic parameters, and the evaluation of ligand specificity effects on triplex DNA formation.

REFERENCES

1. Tyagi, S., and Kramer, F. R. (1996) *Nat. Biotechnol. 14*, 303−308.
2. Tyagi, S., Marras, S. A. E., and Kramer, F. R. (1998) *Nat. Biotechnol. 18*, 1191−1196.
3. Lewin, S. R., Vesanen, M., Kostrikis, L., Hurley, A., Duran, M., Zhang, L., Ho, D. D., and Markowitz, M. (1999) *J. Virol. 73*, 6099−6103.
4. Sokol, D. L., Zhang, X., Lu, P., and Gewirtz, A. M. (1998) *Proc. Natl. Acad. Sci. U.S.A. 95*, 11538−11543.

5. Vet, J. A. M., Majithia, A. R., Marras, S. A. E., Tyagi, S., Dube, S., Poiesz, B. J., and Kramer, F. R. (1999) *Proc. Natl. Acad. Sci. U.S.A. 96*, 6394−6399.
6. Kostrikis, L. G., Tyagi, S., Mhlanga, M. M., Ho, D. D., and Kramer, F. R. (1998) *Science 279*, 1228−1229.
7. Giesendorf, B. A., Vet, J. A. M., Tyagi, S., Mensink, E. J., Trijbels, J. J., and Blom H. J. (1998) *Clin. Chem. 44*, 482−486.
8. Marras, S. A., Kramer, F. R., and Tyagi, S. (1999) *Genet. Anal. 14*, 151−156.
9. Piatek, A. S., Tyagi, S., Pol, A. C., Talenti, A., Miller, L. P., Kramer, F. R., and Alland, D. (1998) *Nat. Biotechnol. 16*, 359−363.
10. Thomas, T. J., Faaland, C. A., Gallo, M. A., and Thomas, T. (1995) *Nucleic Acids Res. 23*, 3594−3599.
11. Thomas, R. M., Thomas, T., Wada, M., Sigal, L. H., Shirahata, L. H., and Thomas, T. J. (1999) *Biochemistry 38*, 13328−13337.
12. Gewirtz, A. M., Sokol, D. L., and Ratajczak, M. Z. (1998) *Blood 92*, 712−736.
13. Agrawal, S., and Zhao, Q. (1998) *Curr. Opin. Chem. Biol. 2*, 519−528.
14. Maher, L. J., 3rd. (1996) *Cancer Invest. 14*, 66−82.
15. Giovannangeli, C., and Hélène, C. (1997) *Antisense Nucleic Acid Drug Dev. 7*, 413−421.
16. Nakashima, S., Matsuura, N., Nagatsugi, F., Maeda, M., Sasaki, S. (1997) *Nucleic Acids Symp. Ser. 37*, 33−34.
17. Nagel, K. M., Holstad, S. G., Isenberg, K. E. (1993) *Pharmacotherapy 13*, 177−88.
18. Shafer, R. H. (1998) *Prog. Nucleic Acid Res. Mol. Biol. 59*, 55−94.
19. Arber, N., Gammon, M. D., Hibshoosh, H., Britton, J. A., Zhang, Y., Schonberg, J. B., Roterdam, H., Fabian, I., Holt, P. R., and Weinstein, I. B. (1999) *Hum. Pathol. 30*, 1087−92.
20. Vos, C. B., Ter Haar N. T., Peterse, J. L., Cornelisse, C. J., and van de Vijver, M. J. (1999) *J. Pathol. 187*, 279−284.
21. Wilcken, N. R., Prall, O. W., Musgrove, E. A., and Sutherland, R. L. (1997) *Clin. Cancer Res. 3*, 849−854.
22. Wang, T. C., Cardiff, R. D., Zukerberg, L., Lees, E., Arnold, A., and Schmidt, E. V. (1994) *Nature 369*, 669−6671.
23. Kim, H., and Miller, D, M, (1998) *Biochemistry 37*, 2666−2672.
24. Plum, G. E., and Breslauer, K. J. (1995) *J. Mol. Biol. 248*, 679−695.
25. Xodo, L. E., Manzini, G., and Quadrifoglio, F. (1998) *Antisense Nucleic Acid Drug Dev. 8*, 477−488.
26. Grant, K. B., and Dervan, P. B. (1996) *Biochemistry 35*, 12313−12319.
27. Shindo, H., Torigoe, H., and Sarai, A. (1993) *Biochemistry 32*, 8963−8969.
28. Yang, M., Ghosh, S. S., and Millar D. P. (1994) *Biochemistry 33*, 15329−15337.
29. Aich, P., Ritchie, S., Bonham, K., and Lee, J. S. (1998) *Nucleic Acids Res.* 26, 4173−4176.
30. http://www.molecular-beacons.org.
31. Bloomfield, V. A., Crothers, D. M., and Tinoco, I., Jr. (2000) *Nucleic Acids: Structures, Properties and Functions*, University Science Books, Sausalito, CA.
32. Postel, E. H., Flint, S. J., Kessler, D. J., and Hogan, M. E. (1991) *Proc. Natl. Acad. Sci*. U.S.A. *88*, 8227−8231.
33. Ebbinghaus, S. W., Gee, J. E., Rodu, B., Mayfield, C. A., Sanders, G., Miller, D. M. (1993) *J. Clin. Invest. 92*, 2433−2439.
34. Igarashi, K., Koga, K., he, Y., Shimogori, T., Ekimoto, H., Kashiwagi, K., and Shirahata, A. (1995) *Cancer Res. 55*, 2615−2619.
35. Bonnet, G., Tyagi, S., Libchaber, A., and Kramer, F. R. (1999) *Proc. Natl. Acad. Sci. U.S.A. 96*, 6171−6176.
36. Thomas, T., and Thomas, T. J. (1993) *Biochemistry 32*, 14068−14074.
37. Musso, M., Thomas, T., Shirahata, A., Sigal, L. H., Van Dyke, M. W., and Thomas, T. J. (1997) *Biochemistry 36*, 1441−1449.
38. Hampel, K. J., Crosson, P., and Lee, J. S. (1991) *Biochemistry 30*, 4455−4459.
39. Singleton, S. F., and Dervan, P. B. (1993) *Biochemistry* 32, 13171−13179.
40. Thomas, T. J., and Bloomfield, V. A. (1984) *Biopolymers 23*, 1295−1306.
41. Thomas, T. J., Ashley, C., Thomas, T., Shirahata, A., Sigal, L. H., and Lee, J. S. (1997) *Biochem. Cell Biol. 75*, 207−215.
42. Antony, T., Thomas, T., Shirahata, A., Sigal, L. H., and Thomas, T. J. (1999) *Antisense Nucleic Acid Drug Dev. 9*, 221−231.
43. Plum, G. E., Pilch, D. S., Singleton, S. F., and Breslauer, K. J. (1995) *Annu. Rev. Biomol. Struct. 24*, 319−350.
44. Plum, G. E. (1997) *Biopolymers 44*, 241−256.
45. Scaria, P. V., and Shafer, R. H. (1996) *Biochemistry 35*, 10985−94.
46. Dunitz, J. D. (1995) *Chem. Biol. 2*, 709−712.
47. Petruska, J., and Goodman, M. F. (1995) *J. Biol. Chem. 270*, 746−750.
48. Liu, L., Yang, C., and Guo, Q. X. (2000) *Biophys. Chem. 15*, 239−251.
49. Losi A., Wegener, A. A., Engelhardt, M., and Braslavsky, S. E. (2001) *J. Am. Chem. Soc. 123*, 1766−1767.
50. Breslauer, K. J., Remeta, D. P., Chou, W. Y., Ferrante, R., Curry, J., Zaunczkowski, D., Snyder, J. G., and Marky, L. A. (1987) *Proc. Natl. Acad. Sci. U.S.A. 84*, 8922−8926.
51. Lavelle, L., Fresco, J. R. (1995) *Nucleic Acids Res. 23*, 2692−2705.
52. Duguid, J. G., Bloomfield, V. A., Benevides, J. M., and Thomas, G. J., Jr. (1996) *Biophys. J. 71*, 3350−3360.
53. Vallone, P. M., and Benight, A. S. (2000) *Biochemistry 39*, 7835−7846.
54. Marras, S. A., Kramer, F. R., and Tyagi, S. (1999) *Genet. Anal. 14*, 151−156.
55. Mergny, J. (1999) *Biochemistry 38*, 1575−1581.
56. Ota, N., Hirano, K., Warashina, M., Andrus, A., Mullah, B., Hatanaka, K., and Taira, K. (1998) *Nucleic Acids Res. 26*, 735−743.
57. Aich, P., Thomas, T. J., and Lee, J. S. (2000) *Nucleic Acids Res. 28*, 2307−2310.

BI010397Z